

# The Orbiter: Pushing the Boundaries of Amateur Rocketry

Yash Malik<sup>1</sup>

*Florida Institute of Technology, Melbourne, Florida 32901, United States of America*

Each amateur rocket has a defining feature or responsibility for being flown, whether it is meant to test avionics, be flight certified, or act as proof of concept. The *Orbiter*, due to its unique design and requirements, was designed as a proof-of-concept rocket. The requirements stated as: the *Orbiter* shall have 80% of the parts be self-built, it shall meet all rules set by the National Association of Rocketry (NAR) pertaining to a Level 2 rocket and Federal Aviation Administration (FAA) requirements, and the rocket shall reach a minimum apogee of 10,000 feet. Since these requirements are quite intensive, extensive planning and analysis was done before manufacturing. Trade analyses were utilized to select the materials, motor, and recovery system. Open Rocket was used for basic simulation of the rocket during its flight. For an in-depth simulation of the *Orbiter* flight, MATLAB was used. To help with the material selection and determining the drag force throughout the flight, ANSYS static structural and CFD was utilized. Manufacturing began once the necessary preparation had been done. While the primary goal of the *Orbiter* is to push the boundary of conventional amateur rocketry, it was also designed as a way for future readers to acquire knowledge and be able to improve upon the errors made.

## I. Nomenclature

$C_D$	=	rocket drag coefficient
$q$	=	dynamic pressure
$\rho$	=	fluid density
$v$	=	object velocity
$A$	=	reference area
$F_D$	=	drag force
$a_{max}$	=	maximum acceleration
$C_{dn}$	=	nose cone drag coefficient
$C_d$	=	parachute drag coefficient
$T_s$	=	static temperature
$T_o$	=	stagnation temperature
$\rho_o$	=	stagnation density
$\rho_s$	=	static density
$P_{op}$	=	operating pressure
$P_s$	=	static pressure
$P_o$	=	stagnation pressure
$m$	=	rocket mass
$T_{max}$	=	maximum thrust
$\gamma$	=	specific heat ratio
$R$	=	gas constant

---

<sup>1</sup> Undergraduate Student, Department of Aerospace, Physics and Space Sciences, and AIAA Student Member (1600792).

## II. Introduction

Every year, NAR holds hundreds of amateur rocket launches, where the rockets that are built and launched hold objective-specific tasks, which can range from certification to proof-of-concept or to a test flight. The *Orbiter* was designed to push amateur rocketry's boundaries. To achieve this goal, three requirements were set. First, the *Orbiter* shall meet all NAR and FAA rules and regulations, emphasizing the Level 2 (L2) rocket rules set in place by NAR. Rules pertaining to an L2 rocket are as follows: the rocket shall contain a J, K, or L class motor, it shall have active recovery and reasonable stability and shall have a certified motor by NAR or another organization with similar standards and a certification program<sup>2</sup>. Due to the FAA's classification of rockets, the *Orbiter* falls into the Class 2 rocket category since it contains certain parts, a high total impulse, and achieves a high altitude. As it did not meet any of the Class 1 requirements<sup>3</sup>, it had to be launched with an FAA certificate of authorization (COA). Secondly, the *Orbiter* shall have 80% of the rocket be self-built, which includes all major components such as the nose cone, avionics bay, and motor. Finally, the minimum altitude target is set at 3,048 meters (m), which will be verified by an altimeter. While the *Orbiter* does not look like a typical L2, it is important to understand the characteristics of one. Typical L2 designs can consist of through-the-wall fins, a body tube diameter greater than the motor tube diameter, and an active recovery system however, these characteristics do not define all L2s. This paper covers the following sections about the *Orbiter*: design, analysis, manufacturing, preflight, testing, and flight analysis.

## III. Design

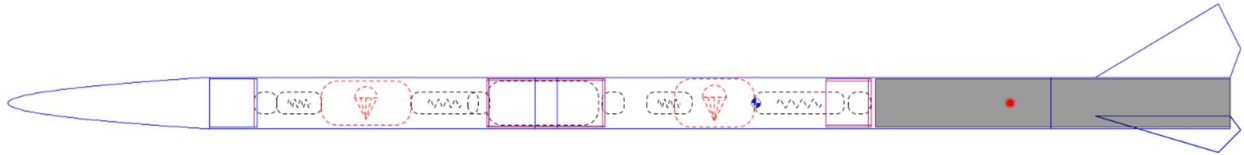


**Fig. 1: The Orbiter Design**

A high-performance rocket (HiPER) is a type of rocket that is characterized by its speed. Typically, it falls between the Mach 1 and 2 range; from the design, it was determined that the *Orbiter* fell into this class. Its HiPER classification meant it would experience higher-than-normal forces, so it would have to be designed differently from a typical L2. The system overview of the *Orbiter* is shown in Fig. 1 where all sections shall be discussed. To maintain the structural integrity of the *Orbiter* a factor of safety of 1.5 would be designed into the rocket.

### A. Motor Choice

The minimum altitude target made it necessary to first select a motor. As per NAR L2 rules, the allowable motors were J, K, or L class motors. Each motor has its own total impulse class limits where J is from 641 N\*s to 1280 N\*s, K is from 1281 N\*s to 2560 N\*s, and L is from 2561 N\*s to 5120 N\*s. Furthermore, the motor dimensions would change based on the impulse of the motor where J is 38 mm or 54 mm, K is 54 mm or 75 mm, and L is 75 mm or 98 mm in diameter. In addition, the higher the impulse in that specific diameter, the longer the motor will get. To determine which of these motor classes would be used, a weighted matrix, Table 1, was utilized.

**Table 1: Motor Class Selection**

Motor Class		J		K		L	
Criteria	Importance	Rating	Weighted Rating	Rating	Weighted Rating	Rating	Weighted Rating
Diameter Range	30%	1	0.3	3	0.9	4	1.2
Cost	35%	4	1.4	3	1.05	1	0.35
Total Impulse	20%	4	0.8	3	0.6	2	0.4
Length	15%	2	0.3	3	0.45	5	0.75
Total	100%		2.8		3		2.7

<sup>2</sup> Other certification programs include the Canadian Association of Rocketry and the Tripoli Rocket Association

<sup>3</sup> Class 1 requirements include: no more than 125 grams propellant; use of a slow burning propellant, made of paper, wood, or breakable plastic; Contains no substantial metal parts; weighs no more than 1,500 grams, including propellant.

The selection of the motor class is shown in Table 1. The criteria evaluated the most important factors that would directly affect the *Orbiter*. Based on the results, a K-class motor with a diameter of 54 millimeters (mm) was chosen as it would maximize space and stay under the COA that had been issued. Due to limited motor availability at the time, a choice of Reloadable Motor System (RMS) K805G-P was used as it was available in the diameter needed. The motor's "P" designation meant it would be plugged, so ejection charges were needed. In addition, the motor made use of an RMS 54/1706 case from AeroTech. Due to the thrust and total impulse provided by the manufacturer, 3,048 m would not be possible with conventional L2 designs. The thrust curve of the motor in relation to the design of the rocket meant that the rocket would have higher forces on launch.

## B. Airframe

As mentioned above, the motor's characteristics heavily influenced the design. The main materials explored were cardboard, fiberglass, and carbon fiber. The criteria that the materials were evaluated on were safety, workability, and useability. While the body tubes could easily be purchased, manufacturing these tubes was necessary as the 80% requirement was hard to meet. Cardboard was decided against as it required more specialized equipment to manufacture. Carbon fiber would be the best as it has the strongest properties but radio-frequency blocking properties and safety concerns<sup>4</sup> did not make it a good choice. This left fiberglass as the only option as it was the strongest material based on the criteria. Fiberglass cloth<sup>5</sup> was used to make the tubes. The weight of the fiberglass was chosen based on a recommendation by the staff at the L3Harris Student Design Center (L3HSDC). The weight decided on was 6 ounces as it was easy to work with and was strong enough. From the motor's characteristics, the airframe's diameter had to be barely big enough for the motor case to fit in, making it a minimum-diameter rocket. This design prevented the construction of through-the-wall fins and caused major space constraints.

The fins were designed to maximize performance and stability. In rocketry, the fins optimize stability throughout the flight and help to maintain an upward orientation. Mounting the fins would pose a challenge as they would not be mounted through the wall, so a new approach had to be taken. The idea was to do an on-the-wall mounting. The method for making the fins was to use a mold such as Polylactic Acid (PLA) or Polyethylene Terephthalate Glycol (PETG), affix it to the body tube using super glue or epoxy, then apply fiberglass repeatedly using different techniques to make a robust fin that would be combined with the body tube.

Space constraints were an issue for the *Orbiter*. Different options were explored to manufacture the avionics bay, such as fiberglass or 3D-printed materials. The main challenge with 3D-printed materials is that the material properties are lower than those of fiberglass. In addition, a pressure hole was needed in the switch band<sup>6</sup>. This meant that there would be a concentrated load along that hole. To increase the strength of the avionics bay, holes were designed into the geometry for 3D printing. The material selection will be discussed later in the paper, as analysis is needed.

## C. Motor Retention System

Due to the *Orbiter's* minimum diameter, a custom motor retention system (MRS) was designed. As the assembly was a big part of retaining the motor and holding the fin can together, it was decided to fabricate it so the MRS would count towards the 80% requirement. Inspiration was taken from existing products, and a design was drafted. The design utilized an AeroTech threaded forward closure to keep the motor retained. It was designed to use a tube with a circular plate that had a hole for an eyebolt to slide into the center of the plate. To prevent the eyebolt from falling out a locking nut would be screwed on the opposite end.

## D. Nose Cone

Completion of the external portion of the *Orbiter* concluded with the nose cone. With many nose cone shapes it would be difficult to select the proper one. So, to select a nose cone geometry from the many types available, Fig. 2 was utilized. Another parameter that would be important in selecting a proper nose cone was the aspect ratio. When the velocity exceeds the speed of sound, the aspect ratio has a larger effect on the  $C_{dn}$  than the geometry. For HiPERs, the aspect ratio is generally considered at least 5:1 or less. To accurately determine the best geometry of the nose cone with an aspect ratio that would be suitable for the *Orbiter*, OpenRocket was utilized.

---

<sup>4</sup> Carbon Fiber is especially dangerous as the fibers can get into the lungs and eyes and remain there for life, potentially causing complications later in life.

<sup>5</sup> Using fiberglass cloth is not uncommon when making a tube coupler; however, it typically uses a non-removable 3D-printed tube, so a new challenge was presented.

<sup>6</sup> The switch band is the section that sticks out from the tube coupler and is in line with the outside of the body tube.

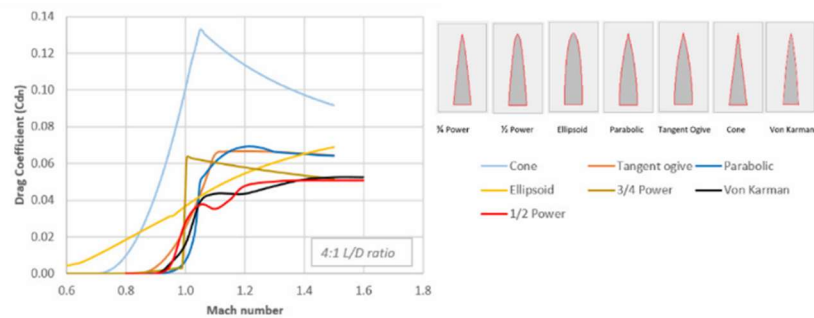


**Fig. 2:  $C_{dn}$  vs. Mach Number [4]**

Based on Fig. 2, it was determined that the best nose cone geometry was ellipsoid,  $\frac{1}{2}$  power series, and tangent ogive. Due to the rocket’s diameter being fixed, the aspect ratio was solely affected by the length of the nose cone. The optimal length was chosen to be 0.275 m as this allowed for a ratio of 87:20. To narrow down between the three choices, a weighted matrix, Table 2, was used, as it would consider all the major criteria that would be needed in designing a good nose cone. The *Orbiter’s* speed meant that there would be more forces as well as some aerothermal heating. An analysis had to be conducted to accurately determine the max aerothermal heating and max  $q$ . All of which is covered in the analysis section.

**Table 2: Nose Cone Geometries**

Nose Cone Geometries		Tangent Ogive		$\frac{1}{2}$ Power Series		Ellipsoid	
Criteria	Importance	Rating	Weighted Rating	Rating	Weighted Rating	Rating	Weighted Rating
Aspect Ratio	40%	1	0.4	4	1.6	3	1.2
$C_{dn}$ vs. Mach No.	30%	2	0.6	3	.9	2	0.6
Max altitude	10%	4	0.4	3	0.3	2	0.4
Max Speed	20%	3	0.6	3	0.8	2	0.75
Total	100%		2		3.6		2.4

### E. Avionics Sled

The avionics sled consisted of an altimeter, batteries, and a global positioning system (GPS). These all would be used in conjunction to recover the rocket successfully. A Stratologger SL100 was used, as it utilized a barometric pressure sensor with an accelerometer failsafe for speeds over Mach 1. This feature, “*MachLock*” was important as the overall speed determined from the OpenRocket simulation showed it was expected to be over Mach 1 for multiple seconds. The GPS that was utilized was a TeleGPS by Altus Metrum. Previous use of this GPS made it the ideal candidate. In addition, to track the descent of the *Orbiter*, an antenna would be used, which was different from the point and track GPSs. The batteries that would be used were two 9-volt batteries, each with a maximum capacity of 1,000 milliamp hours. The two batteries created separate systems, which created a failsafe to prevent them from draining the battery before, during, or after launch. The sled design had to hold everything as well as prevent short-circuiting of the electronics, so the batteries were isolated on one side, and the electronics were on the opposite side.

### F. Recovery System

The *Orbiter’s* recovery system comprised of shock cords, parachutes, quick links, and swivels. Some options for the shock cord were a nylon-Kevlar mix of shock cords and fully Kevlar shock cords. The Kevlar would need to be in places where an ejection charge would be to prevent burning. The nylon would be used for all other ropes. It was decided that an all-Kevlar shock cord would be used to prevent any ejection charge from burning the recovery system. The strength of the Kevlar was decided to be the force of deployment if it were to occur at terminal velocity. While this was the worst scenario, it helped ensure safe operations. The quick links and swivels were determined the same way but did not exceed the strength of the Kevlar, as there would be no added benefit.

Parachute selection was split into two categories: drogue and main chute. To select the drogue and main chute, it’s important to understand the locations at which they deploy and the forces they experience. The drogue chute deploys at apogee, while the main chute deploys at a predetermined altitude. A deployment at apogee meant that there would

be minimal forces, whereas the main chute would have a snatch force. A parachute that descended faster with minimal drifting was preferred for the drogue chute. The parachutes considered for this task were the Cruciform and Tarc-style parachutes. The cruciform was good for high stability as it allowed for a rocket to deploy at slightly faster speeds and not drift as far. The Tarc-style was built upon the cruciform as it had a higher  $C_d$ . In addition, the Tarc-style had fewer shroud lines, with only three strong lines. Therefore, the best choice for the rocket was a Tarc-style parachute for the drogue chute. The main chute would need a slower descent rate, so a larger, slightly more robust parachute was needed. Parachutes considered were sheet, elliptical, spherical, and toroidal parachutes. Each had their own strengths and weaknesses. The best selection for the *Orbiter* was a sheet chute. The main chute had a diameter of 0.99 m with a 106 mm spill hole, which would assist with a stable and faster descent.

#### IV. Analysis

##### A. OpenRocket

Model rocket enthusiasts use OpenRocket to design their rockets and model the altitude. The only issue is that the program becomes more inaccurate for a rocket over Mach 1. The calculations done in OpenRocket use Barrowman's Method. This brings up an issue as the compressible equations used, as they are modifications to the existing equations.

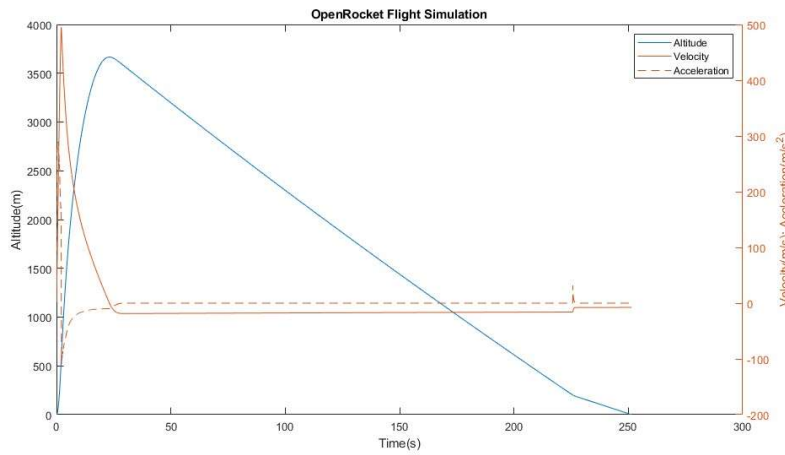


Fig. 3: Flight Simulation

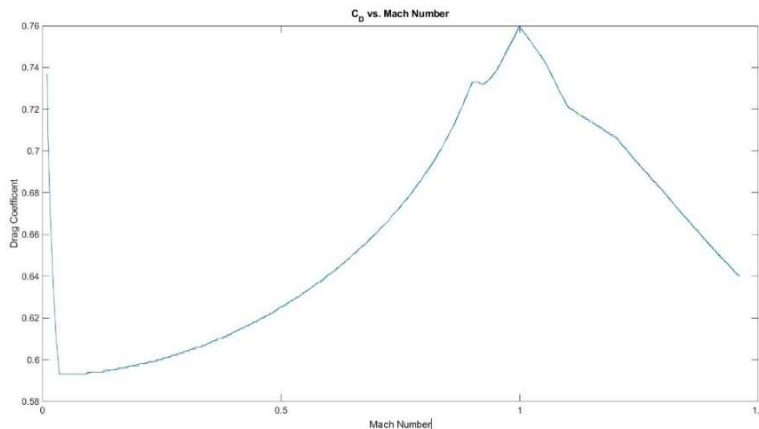


Fig. 4:  $C_D$  vs. Mach Number from OpenRocket

In Fig. 3 and Fig. 4 the model of the *Orbiter* in flight and a  $C_d$  vs. Mach number is plotted. To prove Fig. 3 as valid, a comparison of the drag force at various locations that were tested with another software. ANSYS Fluent was utilized to do this as it uses numerical integration, which will be covered in the next subsection. OpenRocket also created a

$C_D$  vs. Mach number where the most drag will be and where the max  $q$  will be. In Fig. 4, the values of the  $C_D$  vs. Mach number are described. At Mach 0.9, it can be observed that the  $C_D$  drops before increasing up to Mach 1, where it then starts to fall off. This drop at Mach 0.9 is reflected in Fig. 2 as it models parts of the  $C_{dn}$  for the power series  $\frac{1}{2}$  nose cone.

## B. ANSYS Fluent

ANSYS Fluent was used to determine the drag force of the entire *Orbiter*. This would prove beneficial as that force would be applied to the rocket's nose cone. In addition, it would prevent structural failure for the avionics bay and provide a maximum temperature for the nose cone. The accuracy of this software would be much better than that of OpenRocket as ANSYS uses numerical integration to calculate and determine  $C_D$ . "Elements" are assigned along the control volume and the control surface using a geometrical shape that was then used to integrate numerically. While designing the avionics bay for a maximum drag force may seem unrealistic, the rocket's success would need for it to not structurally fail.

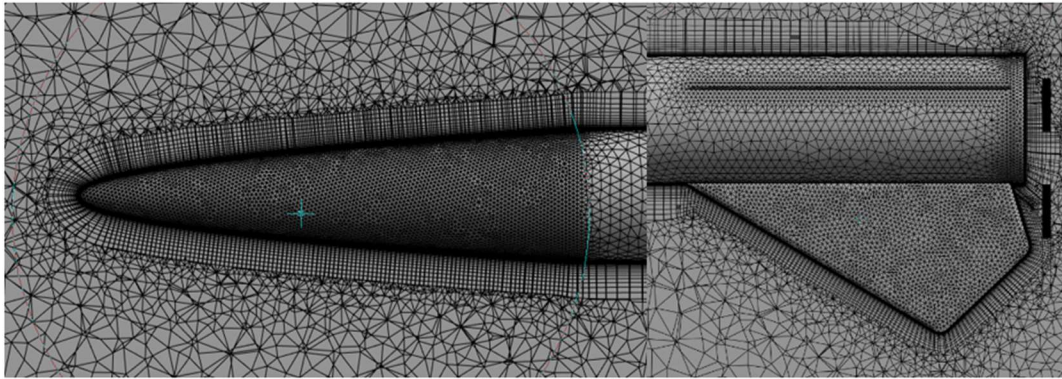


**Fig. 5: Meshing of Nose Cone and Fins**

Two simulations were used for subsonic and supersonic flow. A face meshing of 0.04 meters (m) was used for the subsonic flow. The rocket meshing did not need to be fine as the results would not change much. Inflation layers were utilized using a  $y+$  spacing of 0.0001 m as the first layer thickness from the rocket's wall. In addition, body sizing was applied with a mesh size of 0.1m as the detail needed to be around the model. A density-based K-Omega SST was used to model the turbulent flow accurately with the energy equation. This model gave the ability to model turbulent flow at subsonic speeds as well as handle some compressible effects as it reached the transonic regime.

The simulation for supersonic modeling as the rocket mesh needed to be refined. The rocket walls used two types of face sizing to accelerate meshing and simulation speed. The first sizing was specified for the main airframe, excluding the rocket's fins and nose cone. The second meshing was the fins and nose cone, with it having a much more refined meshing than the main airframe with a sizing of 0.002 meters. The solution would change as supersonic speeds are reached; the bounds turn from velocity inlet to pressure inlet. In addition, the model changes from a K-Omega SST model to a K-Epsilon Realizable model. The isentropic equations and Table A.2[11] were used to determine the total and static pressure needed.

$$\frac{T_0}{T_s} = 1 + \frac{\gamma-1}{2} M^2 \quad (1)$$

$$\frac{P_0}{P_s} = \left(\frac{\rho_s}{\rho_0}\right)^\gamma = \left(\frac{T_0}{T_s}\right)^{\gamma/(\gamma-1)} \quad (2)$$

$$\rho = \frac{P_s + P_{op}}{RT_s} \quad (3)$$

$$\frac{P_0 + P_{op}}{P_s + P_{op}} = \left(1 + \frac{\gamma-1}{2} M^2\right)^{\gamma/(\gamma-1)} \quad (4)$$

The equations were needed to calculate the static and stagnation pressure required for the pressure inlet, pressure outlet, and pressure far field. Where  $P_{op}$  is the operating pressure of 101,325 Pascals (Pa),  $\gamma$  is 1.4 for dry air, R is the

gas constant of air 287 J/kg\*K, and total density is 1.225 kg/m<sup>3</sup>. The total pressure was determined to be 270,639 Pa and a static pressure of 101,325 Pa. The total temperature was determined to be 299 K.

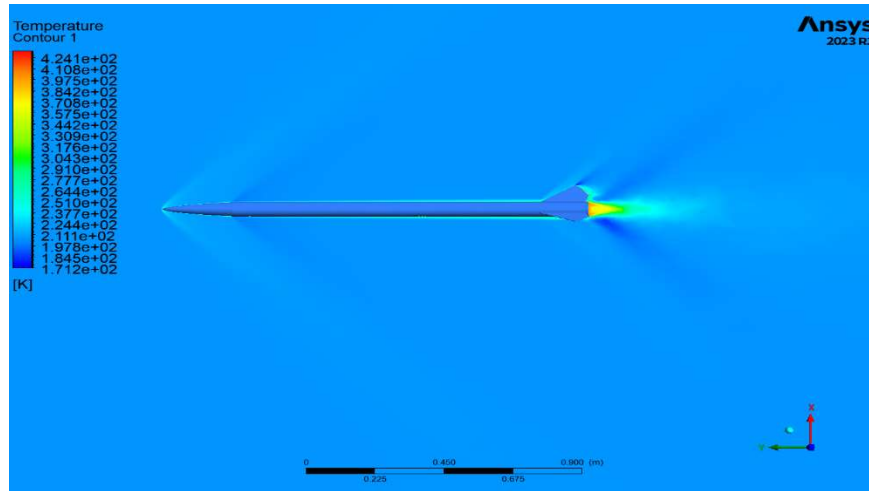


**Fig. 6: Supersonic Flow Over the *Orbiter***

Once the solution converged, it was determined that the max temperature of 424.1 K (Fig. 6) at the tip would need to survive for it not to catastrophically fail. A weighted matrix (Table 3) was used to determine the appropriate material for the nose cone. This matrix compares all the properties of the materials being looked at. The selected material would be nylon-reinforced carbon fiber (PA-6).

**Table 3: Nose Cone Material Selection**

Nose cone		PLA		PA-6 CF		Polycarbonate	
Criteria	Importance	Rating	Weighted Rating	Rating	Weighted Rating	Rating	Weighted Rating
Heat Deflection Temp.	25%	1	0.25	4	1	2	0.5
Impact Strength	15%	1	0.15	2	0.3	3	0.45
Compressive Strength	20%	3	0.6	3	0.6	2	0.4
Cost	10%	5	0.5	4	0.4	3	0.3
Ease of Printing	20%	5	1	4	0.8	2	0.4
Post Printing Extra work	10%	5	0.5	3	0.3	2	0.2
Totals	100%		3		3.4		2.25

### C. ANSYS Static Structural

The deformation that the avionics bay would undergo was a concern that was addressed. The tube coupler would combine both halves of the *Orbiter* to prevent it from splitting<sup>7</sup> prematurely during flight. Materials from Table 4, were looked at for their structural properties. A static structural model in ANSYS (Fig. 7) was used to determine the deformation that would be experienced. As it did not have complex geometry, refined mesh was unnecessary, so a mesh sizing of 0.002 m. Based on all the materials that were considered they were all inputted into the simulation, with the selected material PA-6 CF.

The analysis determined that the deformation experienced was the greatest at the switch band and continued to drop as it reached the edges of the bay. In addition, based on the deformation method, it would cause either compression or tension in the switch band, potentially depending on its orientation, a stress concentration in the hole for pressure sampling.

<sup>7</sup> In this case, the splitting that would be experienced was flexural bending.

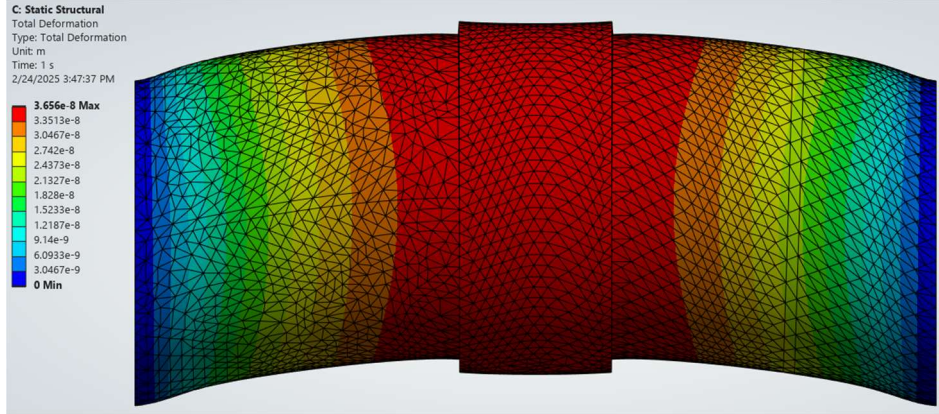


**Fig. 7: Total Deformation of Avionics Bay**

**Table 4: Avionics Bay Material Selection**

Avionics Bay		PLA		PA6-CF		ONYX	
Criteria	Importance	Rating	Weighted Rating	Rating	Weighted Rating	Rating	Weighted Rating
Bending Strength	25%	1	0.25	3	0.75	4	1
Impact Strength	10%	1	0.1	3	0.3	4	0.4
Compressive Strength	20%	2	0.4	3	0.6	4	0.8
Cost	10%	5	0.5	4	0.4	2	0.2
Ease of Printing	20%	5	1	4	0.8	2	0.4
Post Printing Work	15%	5	0.75	3	0.45	3	0.45
Total	100%		3		3.3		3.25

#### D. Calculations

To ensure that the *Orbiter's* parachute would survive as the main chute deployed, a snatch force calculation was done. To validate the OpenRocket information a max acceleration calculation was done.

$$F_D = \frac{1}{2} \rho v^2 C_d A \quad (5)$$

$$a_{max} = \frac{T_{max} - F_D}{m} \quad (6)$$

To calculate the maximum acceleration, eq. 6 was used and determined to be 275m/s<sup>2</sup>. This value was an underestimation. So, any values taken from OpenRocket would be considered an overestimation. The calculated snatch force was determined to be 100 N using eq. 6. This equation also assumed that it would immediately deploy.

#### V. Manufacturing

Once design and analysis were completed, manufacturing began. Body tube manufacturing was the first to begin. As body tube manufacturing in this method has very few resources, an approach like filament winding was taken. The process utilized a mandril was 3D-printed out of PLA and fiberglass cloth was wrapped around it. To bond the fiberglass together, West Systems 105 Resin with West Systems 206 hardener was used. This was selected as it was readily available in L3HSDC, where most manufacturing occurred. Car wax was used to prevent the airframe from sticking to the mandril. Some errors in the manufactured first body tube were due to the mandril. The way the PLA was attached created an issue that caused the mandril to bend from the weight of the fiberglass and epoxy. In the second iteration made for the *Orbiter's* booster section, a metal rod was slid through the mandril to allow for the weight of the wet body tube to not bend it.

Once the body tubes were manufactured, a model of the fins was 3D-printed to be used as a mold. The primary material used for this was PETG. After it was printed, it was then affixed to the model using a 3D-printed Fin aligner using superglue as it was not supposed to bear any structural strength but rather act as a mold. From there, a fillet was



created using spherical phenolic micro-balloons. This created the desired shape for epoxying the fiberglass cloth onto it.

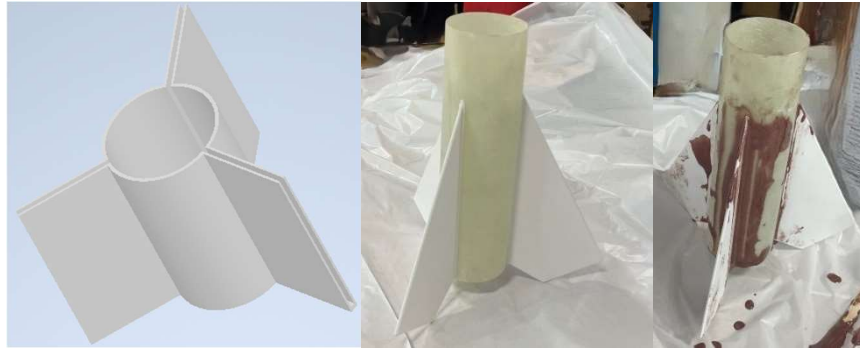


**Fig. 8: Fins Aligner, and Fins at Different Stages**

The 3D-printed aligner, the attachment, and the micro-ballooned fins are shown in Fig. 8. The fiberglass was then applied to the fins, and they combined into the body tube. This made sure that the fins were as strong as possible while minimizing weight.

Once the airframe was completed, the motor retention system was manufactured. To make this, an aluminum 6061 tube was acquired. The dimensions of the tube were not exact, so it was machined down. The disk that would act as the retaining ring for the eyebolt needed to be welded. A 3/8th inch eye bolt was then put in the retaining ring and was tightened using a locking nut. It was then attached to the rocket using West Systems epoxy and hardener mentioned above.

The nose cone and the avionics bay were 3D-printed using PA-6 CF which was determined in the previous section. Print-in-place nuts were added to the shoulder of the nose cone while printing. This would securely attach the nose cone to the rest of the rocket. To mount the recovery harness to the nose cone and avionics bay, a combination of 1/4 eye nuts and a 1/4 threaded rods were used.

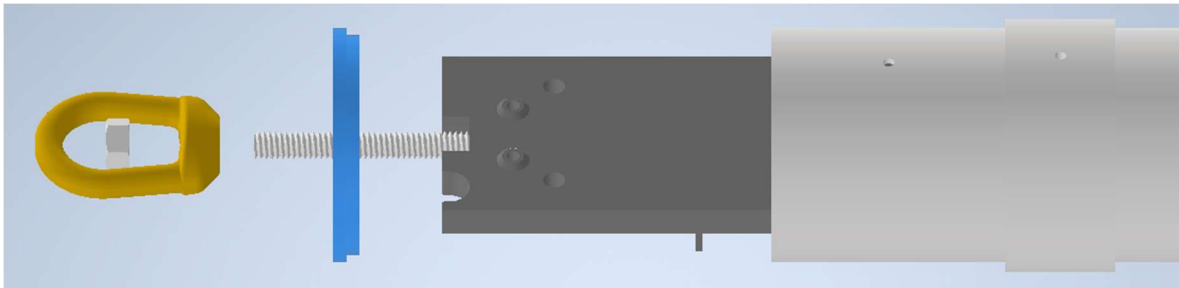


**Fig. 9: Avionics Exploded View**

The avionics sled was also 3D-printed. It was made from PETG, with a tolerance of 0.1mm between the sled and the bay, allowing for a more rigid avionics bay. The nose cone and avionics bay bulkheads were manufactured out of aluminum 6061 using a waterjet. Holes were drilled in for the ejection wires and bolts to ensure the bulkheads would not spin and for the TeleGPS's antenna to stick out. In Fig. 9, the avionics assembly is shown where the bulkhead, eyebolt, and nut are mirrored on the opposite side.

The majority of recovery system manufacturing was cutting ropes to length to create a recovery harness and tying knots. The lengths chosen were double the length of the section it would be in, plus some extra to account for the knots that would be needed. The parachute deployment bags would be attached to a location closer to the body tube, while the parachute would be attached closer to the avionics bay.

## **VI. Testing, Preflight, and Flight**

The testing of the *Orbiter* consisted of an ejection test and testing and programming of the TeleGPS and Stratologger SL100. The programming consisted of the location for the main to deploy at and confirmation that the drogue deployment was activated on the altimeter. Once those two were confirmed, the Stratologger was completed. The TeleGPS was ground tested to ensure that everything worked and that it was operational inside the avionics bay

and far away from the tracking antenna. The final step in the testing phase was ejection testing of the *Orbiter* to determine the charge needed to cause a deployment of parachutes. To make the ejection charges, one end was clamped using Triple Seven and a tube, and the wadding was compressed down. Hot glue was applied to hold the wadding in. From there, the Triple Seven was added. An electronic match was placed in the Triple Seven. Wadding and hot glue were added on the other side. This method of creating charges determined that the charge needed was 20 grains of Triple Seven on both sides.



**Fig. 10: Rocket Assembly**

Preflight preparation consisted of the assembly of the motor, which was done using the instructions provided by AeroTech, as any deviation from them would cause the motor to become uncertified. At the launch site, the charges were created, the TeleGPS was turned on, a flight card was filled out, and then the rocket was placed on the pad shown in Fig. 10. The Stratologger was armed by twisting the switch wires together, with 3 beeps signifying continuity, and the TeleGPS was checked for signal. Once both were confirmed working, the rocket was launched per all FAA and NAR-sanctioned rules, and the COA was active.

As the rocket launched, GPS data being relayed to the antenna and being read by the Altus Metrum app lost connection. In addition, the GPS did not realize that it was in flight. Roughly at 1,200m to 1,500m, the connection to the GPS was re-established, and flight data began recording. However, no parachute event was seen on the GPS telemetry nor visually, with the only data signifying it re-accelerated downwards past the speed it should have been falling while under drogue. After 4-5 hours of searching in various locations near the last recorded location, it was considered an unsuccessful recovery.

## VII. Post Flight Analysis

While the failure of the *Orbiter* cannot fully be determined we can make assumption as to why it failed. The first theory was that no deployment happened, so the rocket went ballistic. Although it had a strong argument, data from the GPS in relation to the OpenRocket data meant that it was unlikely. The second theory was that there was a deployment, but that deployment messed with the GPS data telemetry. This theory was supported as there were issues previously with another rocket launched by an FIT student that was under similar classifications as an L2 had issues with telemetry, although it was considered a once-off as there was no proof that could back it up. This second failure in the GPS was enough to start thinking that maybe it was not a one-off; without other launches in smaller diameter rockets such as this one, a pattern cannot be made. As for the altitude, the height that was recorded by the TeleGPS was recorded to be 2,876m. However, the data could be inaccurate as some information connotated to a large error, which was off by at least 2,000 ft, meant no altitude data could be used.

While the recovery was unsuccessful, conclusions can be drawn about certain parts of the *Orbiter*. The fin can, motor retention system, and fins are considered successes as they all held up to the forces acting on the rocket as it ascended past max  $q$ . The 3D-printed avionics bay was a partial success. While overall the *Orbiter* cannot be considered successful, the construction can be considered successful. The *Orbiter* withstood the launch load during

its boost from the flight. Uncertainty makes it not fully successful as cracks may have formed at any point during the flight, which was only able to be determined from recovery. The airframe and the method of construction can be considered a complete success as the body tubes held up to all the normal flight stress going up. Anything after cannot be concluded. Finally, the nose cone can be considered a partial success as the first half of the flight proved the ability to deflect the heat as it ascended. It cannot be concluded if any melting, large deformations, or cracking formed during flight or from landing.

## VIII. Conclusion

While the *Orbiter* cannot be considered a complete success, it can be considered successful in meeting the main overarching goal of the project: successfully pushing the boundaries of conventional amateur rocketry. It explored new and alternative ways to design, manufacture, and launch a rocket, from making body tubes to simulating and determining the drag and max  $q$  using ANSYS Fluent. While it was unfortunate that the rocket could not be recovered, plans for a future rocket are being made. It will utilize these techniques and knowledge gained from this experience. These lessons learned can help guide those who want to explore new ideas and push the boundaries of conventional amateur rocketry.

## Acknowledgments

Y.M. would like to thank the following individuals and organizations: *Spaceport Rocketry Association* for sharing the launch equipment, rocketry expertise, and for hosting its monthly launches; Dr. Firat Irmak, for his help in validating FEA results, providing advice and his expertise in structures; Dr. Mark Archambault for his assistance in CFD. The L3HSDC staff for their invaluable assistance with 3D printing, providing an open workspace, component materials, and equipment; The Machine Shop at FIT for their assistance in machining and advising for the manufacturing of parts; the Florida Institute of Technology's AIAA chapter advisor, Dr. Danilo de Camargo Branco for his continued support in that chapter and all its functions; and the Florida Institute of Technology's AIAA chapter for sharing their altimeter, motor case, and other materials, as well as all they do to help support their members.

## References

- [1] "HPR Level 2 Certification Procedures – National Association of Rocketry", Jan 2022. URL [https://narocket.club/express.com/content.aspx?page\\_id=22&club\\_id=114127&module\\_id=673088](https://narocket.club/express.com/content.aspx?page_id=22&club_id=114127&module_id=673088)
- [2] "FAA Regulations – National Association of Rocketry", URL [https://www.nar.org/content.aspx?page\\_id=22&club\\_id=114127&module\\_id=668325](https://www.nar.org/content.aspx?page_id=22&club_id=114127&module_id=668325)
- [3] "Fins for Rocket Stability – Richard Nakka's *Experimental Rocketry* Web Site", Aug 2001. URL <https://www.nakka-rocketry.net/fins.html>
- [4] "Nose Cone Design Considerations – Richard Nakka's *Experimental Rocketry* Web Site", July 2023. URL [https://www.nakka-rocketry.net/RD\\_nosecone.html](https://www.nakka-rocketry.net/RD_nosecone.html)
- [5] "Stratologger SL100 User Manual", Perfect Flite, Andover, NH, United States, pp 5.
- [6] "TeleGPS Owner's Manual", Altus Metrum, Black Forest, CO, United States, Aug 2024, pp 22.
- [7] "Rocket Motor Resources – National Association of Rocketry," URL <https://www.nar.org/RocketMotorResources>
- [8] "Certified Motor List – National Association of Rocketry," URL [https://www.nar.org/content.aspx?page\\_id=22&club\\_id=114127&module\\_id=669684](https://www.nar.org/content.aspx?page_id=22&club_id=114127&module_id=669684)
- [9] "High Power Rocket Safety Code – National Association of Rocketry", Aug 2012, URL <https://www.nar.org/HighPowerRocketSafetyCode>
- [10] "Pressure Inlet Boundary Conditions – Ansys Help," Jan 2025. URL [https://ansyshelp.ansys.com/public/account/secured?returnurl=/Views/Secured/corp/v251/en/flu\\_ug/flu\\_ug\\_bcs\\_sec\\_bound\\_cond.html](https://ansyshelp.ansys.com/public/account/secured?returnurl=/Views/Secured/corp/v251/en/flu_ug/flu_ug_bcs_sec_bound_cond.html)
- [11] Anderson, John D. "Modern Compressible Flow With Historical Perspective," 4<sup>th</sup> ed. McGraw Hill, New York, 2021 pp. 30, 712-715
- [12] Niskanen, Sampo "OpenRocket Technical documentation," M.Sc. thesis, Helsinki University of Technology, 2009
- [13] "Onyx Markforged Technical Data Sheet – Markforged," URL <https://markforged.com/materials/plastics/onyx>
- [14] "PA6-CF Technical Data Sheet – Bambu Labs," URL [https://us.store.bambulab.com/products/pa6-cf?srsId=AfmBOoq\\_1BkHqosyYTQtQODLL2aFkPIy0UobFYIxX1ICABAB5jhOxQID](https://us.store.bambulab.com/products/pa6-cf?srsId=AfmBOoq_1BkHqosyYTQtQODLL2aFkPIy0UobFYIxX1ICABAB5jhOxQID)
- [15] "PA6-CF Polyimide Technical Data Sheet – Polymaker," URL <https://polymaker.com/product/polyimide-pa6-cf/>
- [16] "PolyLite PC Technical Data Sheet – Polymaker," URL <https://polymaker.com/product/polylite-pc/>
- [17] "Overture PLA Technical Data Sheet – Overture," URL <https://overture3d.com/collections/3dprinting-pla-collection-overture3d/products/overture-pla-3d-printing-filament-2kg>
- [18] "Overture PETG Technical Data Sheet – Overture," URL <https://overture3d.com/collections/all-filaments/products/overturepla>
- [19] "K805G Thrust Curve – thrustcurve.org," URL <https://www.thrustcurve.org/motors/AeroTech/K805G/>